DOI: 10.1534/genetics.107.084376

Mutations in the Drosophila Mitochondrial tRNA Amidotransferase, *bene/gatA*, Cause Growth Defects in Mitotic and Endoreplicating Tissues

Jason Z. Morris,[1] Leah Bergman, Anna Kruyer, Mikhail Gertsberg, Adriana Guigova, Ronald Arias and Monika Pogorzelska

Department of Natural Sciences, Fordham University, New York, New York 10023

Manuscript received November 9, 2007
Accepted for publication December 5, 2007

ABSTRACT

Rapid larval growth is essential in the development of most metazoans. In this article, we show that *bene*, a gene previously identified on the basis of its oogenesis defects, is also required for larval growth and viability. We show that all *bene* alleles disrupt *gatA*, which encodes the Drosophila homolog of glutamyl-tRNA(Gln) amidotransferase subunit A (GatA). *bene* alleles are now referred to as *gatA*. GatA proteins are highly conserved throughout eukaryotes and many prokaryotes. These enzymes are required for proper translation of the proteins encoded by the mitochondrial genome and by many eubacterial genomes. Mitotic and endoreplicating tissues in Drosophila *gatA* loss-of-function mutants grow slowly and never achieve wild-type size, and *gatA* larvae die before pupariation. *gatA* mutant eye clones exhibit growth and differentiation defects, indicating that *gatA* expression is required cell autonomously for normal growth. The *gatA* gene is widely expressed in mitotic and endoreplicating tissues.

FOR most metazoans, the energy stores available during embryogenesis are sufficient to implement the basic body plan, but not to attain the necessary size for reproductive development. Free-living larvae consume and expend enormous resources to attain appropriate size for adulthood. Larvae grow by increasing cell size and/or cell number in a manner consistent with the needs of the organism and the availability of metabolic factors, including amino acids and energy.

Drosophila larvae increase their mass ~200-fold during the 4-day larval period (Lilly and Duronio 2005). Some larval tissues, including the central nervous system and the imaginal discs, grow via mitotic division, but most larval growth is due to increasing cell size in endoreplicating tissues. Cells in some of these tissues, such as the salivary gland and fat body, increase their DNA content to hundreds of times that of a normal diploid cell and achieve gigantic size. Adult cells that require rapid growth, such as the nurse cells of the ovary, also rely on endoreplication (Edgar and Orr-Weaver 2001).

Multiple mechanisms in the fly control tissue and organism size by coordinating cell growth and cell cycle regulation with developmental programs and with nutritional state. Most of the major intercellular signaling pathways, including Wnt, BMP, Notch, and Hedgehog, locally affect the size of mitotically dividing tissues via control of cell division and/or cell death, but they do not regulate the growth of the endoreplicating tissues that contribute most to larval growth (Britton *et al.* 2002). Organ size is also under the control of the *hippo* pathway, which regulates cell cycle and apoptosis (Saucedo and Edgar 2007). Drosophila size is also regulated by the cell growth/cell cycle regulators dMyc and cyclin D-Cdk4 and by the insulin–Tor-signaling pathway, which acts to coordinate anabolic metabolism and cell growth with nutrient supply (Weinkove and Leevers 2000; Edgar 2006).

Several metabolic factors are essential for normal growth in Drosophila. The translation initiation factor EIF4A regulates Drosophila growth in a dose-dependent manner (Galloni and Edgar 1999). EIF4A was also recently shown to act downstream of the Drosophila BMP homolog, Dpp, in regulating cell growth in the amnioserosa (Li and Li 2006). The *Minute* genes, which have long been known to mediate cell growth and cell competition, encode many cytoplasmic ribosomal proteins (Lambertsson 1998). Mutations in three other cytoplasmic ribosomal proteins, Pixie, RpL5, and RpL38, disrupt wing development downstream of the insulin pathway (Coelho *et al.* 2005). Defects in Bonsai, a mitochondrial ribosomal protein, result in small larvae that exhibit cell proliferation defects (Galloni and Edgar 1999; Galloni 2003). Whether these mutants grow poorly simply due to lack of permissive factors (*e.g.*, efficient translation or energy production) or to instructive signals regulating energy allocation to cell growth is an open question (see discussion).

Mutants in *benedict* (*bene*) were first isolated in a clonal screen in the Drosophila ovary for oogenesis defects

[1]*Corresponding author:* Department of Natural Sciences, Fordham University, 113 W. 60th St., LOW 813, New York, NY 10023.

(Morris *et al.* 2003). All three *bene* alleles isolated in the clonal screen are lethal in *trans* to each other or the deficiency. Egg chambers with homozygous *bene* mutant germ cells arrest in mid-oogenesis. The nurse cell chromosomes in these clones contain less DNA than those in similarly aged heterozygous egg chambers, and they fail to properly transition from polytene to polyploid chromosomal morphology. Instead, the nurse cell chromosomes appear tightly condensed well into mid-oogenesis. *bene* oocyte chromosomes appear stringy and fragmented in contrast with the condensed, spherical karyosome morphology of wild-type oocyte chromosomes (Morris *et al.* 2003). The germ cell clone defects in the ovary were cell autonomous; mutant polyploid nurse cells and meiotic oocytes displayed growth and chromosome morphology phenotypes and other tissues appeared wild type (Morris *et al.* 2003).

In this article, we molecularly identify *bene* as the gene encoding Drosophila glutamyl-tRNA(Gln) amidotransferase subunit A (GatA), a protein required in many prokaryotes and in mitochondria for proper translation of glutamine codons. We therefore rename the *50-40*, *112-38*, and *145-30* alleles isolated in the clonal screen as $gatA^{50}$, $gatA^{112}$, and $gatA^{145}$, respectively. We show that *gatA* mutant larvae exhibit several growth and maturation defects, including molting delays and decreased size of mitotic and endoreplicating tissues. The larvae die before pupariation. Consistent with an essential role in mitochondrial function, we show that *gatA* is expressed widely in many tissues in larvae and adults. We also show by mosaic analysis that *gatA* is required in eyes, as it is in egg chambers, for normal growth.

MATERIALS AND METHODS

Drosophila stocks, culturing and scoring of larvae, and genetic and molecular mapping: Stocks were maintained on standard Drosophila medium at 18°. All fly crosses and stocks for experiments were grown at 25°. The Bloomington Drosophila Stock Center, the Drosophila Stock Center in Szeged, Hungary, and the Lehmann, Treisman, and Johnston labs all provided stocks. The following stocks were used: $gatA^{50}$*/TM3,Sb,* $gatA^{112}$*/TM3,Sb,* $gatA^{145}$*/TM3,Sb, Df(3R)cha*^{7}*,red*^{1}*/TM6B, hs-hid/TM3,Sb, kr-GFP, P{neoFRT}82B, P{lacW}l(3)S092902/TM3,Sb, Df(3R) Exel6182/TM6B, Df(3R)Exel6183/TM6B, w, ey-FLP, Gla-lacZ; FRT Rps3, P{ubi-GFP,* and *w+ }/ TM6B.*

All *gatA* alleles and *Df(3R)cha*^{7}*,red*^{1} were balanced over *TM3,Sb,kr-GFP* using *hs-hid/TM3,Sb,kr-GFP.* Genetic mapping was carried out by complementation testing for lethality. Point mutants were further complementation tested for larval growth defects. For phenotypic analysis, *gatA/TM3,Sb,kr-GFP* alleles were crossed to each other or to *Df(3R)cha*^{7}*,red*^{1} and permitted to lay eggs for 2–3 hr at 25°. Embryos were then permitted to develop at 25° for 1–6 days. Larvae were scored as *gatA/+*, *gatA/gatA*, or *gatA/Df* by the presence or absence of GFP in fluorescence microscopy. Larvae were staged by mouth-hook morphology under transmitted light microscopy and photographed using a Nikon Eclipse 50i microscope and a Photometric Coolsnap EZ camera.

Mapping of the *P{neoFRT}82B P{lacW}l(3)S092902* insertion point by inverse PCR was carried out as described (Bellen *et al.* 2004). PCR templates were sequenced (Fisher) and analyzed using DNAStar software. Sequences were compared to the Drosophila genome by BLAST (Altschul *et al.* 1990) and aligned with ClustalW (Chenna *et al.* 2003).

Eye clones: *w, ey-FLP, Gla-lacZ; FRT Rps3, P{ubi-GFP, w+ }/ TM6B* females were crossed by *FRT e* $gatA^{50}$*/TM3, Sb* males, *FRT e* $gatA^{112}$*/TM3, Sb* males, or *FRT +/TM3, Sb* males. We submerged adult offspring in 100% ethanol and photographed the eyes with a Zeiss Stemi SV11 Apo microscope and a Zeiss Axio Cam HRc camera.

Immunofluorescence and DAPI staining: Larvae were dissected in Ringers or 1× insect PBS and fixed in 4% formaldehyde in PBS. Subsequent washes were carried out in PBSTr (1× PBS with 1% triton) with the following exceptions: when antibody was used, primary blocking and incubation and subsequent washes were in PBSTrB (PBSTr with 1% BSA). Secondary blocking and incubation was in PBSTrB-S (PBSTrB with 5% normal donkey serum from Jackson Immunoresearch Laboratories). Two micrograms of DAPI was added to the penultimate wash. We photographed samples using a Nikon Eclipse 50i microscope and a Photometric Coolsnap EZ camera.

Allele sequencing and sequence analysis: PCR templates for sequencing of the *gatA*- and *NP15.6*-coding regions were generated using the Expand Hi-Fidelity PCR kit (Boehringer Mannheim, Indianapolis). Products of PCR reactions were purified from agarose gels using the QiaexII kit (QIAGEN, Valencia, CA) and sequenced with gene-specific primers (Fisher). Sequences were assembled and analyzed using the Lasergene DNAStar programs Editseq and Seqman. ClustalW sequence alignments were generated using the DNAStar Megalign program.

Northern blot: We crossed $gatA^{50}$*/TM3,Sb kr-GFP* by $gatA^{112}$*/ TM3,Sb kr-GFP.* Five days after egg laying (AEL) we used the GFP balancer to sort $gatA^{50}$*/*$gatA^{112}$ larvae from *gatA/TM3, Sb kr-GFP.* Total RNA was purified using TRIZOL (Invitrogen, San Diego) and mRNA was purified using the MAG mRNA purification kit (Ambion), using 115 μg total RNA from both larval classes. We ran and blotted the formaldehyde gel using standard techniques and probed the blot sequentially with random-primed ^{32}P probes from PCR templates of *NK15.6* and *RP49.*

RT–PCR: Wild-type larvae were dissected 5 days AEL and the following tissues were isolated: gut (entire), imaginal discs (mixed eye-antennal, leg, and wing), fat body, salivary gland (with some associated fat body), and brain (including optic lobes and ventral ganglia). We also dissected the ovaries from adult females. We purified Trizol (Invitrogen), and we carried out first-strand cDNA synthesis with the Superscript II kit (Invitrogen) and poly(dT) primers. We used the following PCR primers that flank the third intron of *gatA*: sense primer (GACTAAGAACATCTGGAGCG) and antisense primer (CAG ATGTAACCTGGTAAAAGGC).

RESULTS

***gatA* alleles:** Of ~10,000 independent lines generated in an ethyl methanesulfonate (EMS) clonal screen for ovary defects, three alleles, previously denoted *112-38*, *50-40*, and *145-30*, compose the "*benedict*" (*bene*) complementation group (Morris *et al.* 2003). We now denote the alleles $gatA^{112}$, $gatA^{50}$, and $gatA^{145}$ in light of our identification of *gatA* as the gene disrupted in these mutants (see below). We identified several Deficiencies in the Bloomington collection that failed to complement these alleles, including *Df(3R)cha*^{7} *red*^{1}, *Df(3R)Exel6182,*

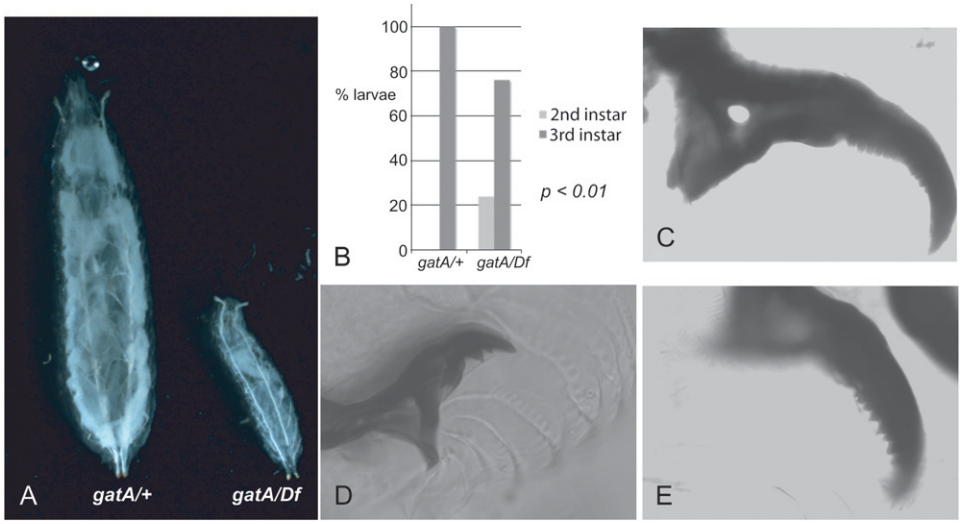

FIGURE 1.—*gatA* growth and maturation defects. All larvae are siblings hatched from eggs collected from the same vial after a 2-hr egg lay. (A) *gatA* larvae are much smaller than wild-type 5 days AEL. (Left) *gatA*/+. (Right) $gatA^{112}$/*Df*. (B) Graph showing delayed molting into third instar larvae of *gatA* mutants. (Left bar) *gatA*/+. (Right bars) $gatA^{112}$/*Df*. (C–E) mouth-hook morphology 5 days AEL. (C) Wild-type third instar larva. (D) $gatA^{112}$/*Df* second instar larva. (E) $gatA^{112}$/*Df* third instar larva.

and *Df(3R)Exel6183*. Complementation tests against the Szeged collection of lethal P insertions that had been mapped to or close to the region defined by these Deficiencies identified a single insertion line, *l(3)S092902*, that failed to complement $gatA^{112}$, $gatA^{50}$, and $gatA^{145}$. We now denote that insertion allele $gatA^{S}$.

***gatA* larval growth and lethality:** We used $gatA^{112}$, $gatA^{50}$, and $gatA^{S}$ and the deficiency, *Df(3R)cha*^{7} *red*^{1}, for most of our phenotypic analysis, and we observed no differences in the phenotypes of $gatA^{S}$ homozygotes or of $gatA^{112}$, $gatA^{50}$, or $gatA^{S}$ in *trans* to *Df(3R)cha*^{7} *red*^{1}. We carried out 2-hr egg lays of the cross *gatA/TM3,Sb, kr-GFP* × *Df/TM3,Sb,kr-GFP* and sorted sibling *gatA*/+ (including *Df*/+) from *gatA/Df* larvae by the presence or absence of GFP. *gatA/Df* larvae do not exhibit any obvious patterning defect, although they grow more slowly than *gatA*/+. By 3–4 days AEL, *gatA/Df* larvae are smaller than their wild-type siblings. By 5 days AEL, some of the *gatA/Df* larvae are dead, and the living larvae are obviously smaller than their siblings (Figure 1A). Wild-type larvae pupariate by the end of the fifth day AEL but the *gatA/Df* larvae do not. *gatA/Df* larvae continue to forage actively on the surface of the food throughout their lives, although in contrast with their wild-type siblings, they rarely burrow into the food. The mutant larvae do not grow significantly beyond day 3 AEL, although some of them live 9 days or longer.

To determine if the larvae were developmentally arrested, developmentally delayed, or merely slow growing, we examined their mouth hooks. By 4 days AEL, the wild-type larvae all had the characteristic mouth-hook morphology of third instar larvae (Figure 1, B and C). In contrast, even on day 5 AEL, only 76% of *gatA/Df* larvae were third instar larvae, and the remaining 24% were second instar larvae ($P < 0.01$) (Figure 1, B–E). The first larval molt is also delayed in *gatA* mutants (not shown). We conclude that mutations in *gatA* arrest growth, delay larval molts, and permit development only as far as the third larval stage. These observations are consistent with the fact that timing of larval molting and pupariation depends on nutrition and growth rates (EDGAR 2006).

***gatA* organ growth defects:** Because we had originally identified *gatA* mutants on the basis of growth and DNA replication defects in mutant nurse cells, we were interested in learning how the sizes of individual tissues were affected in *gatA* mutants. Dissection and DAPI staining of larvae revealed dramatic differences between *gatA*/+ and *gatA/Df* or *gatA/gatA* larvae. Diploid tissues, including imaginal discs (Figure 2, A and B) and brains (Figure 2, C and D), are much smaller in *gatA/Df* 5-day-old larvae than in their wild-type siblings of the same age. Endoreplicating tissues also show strong growth

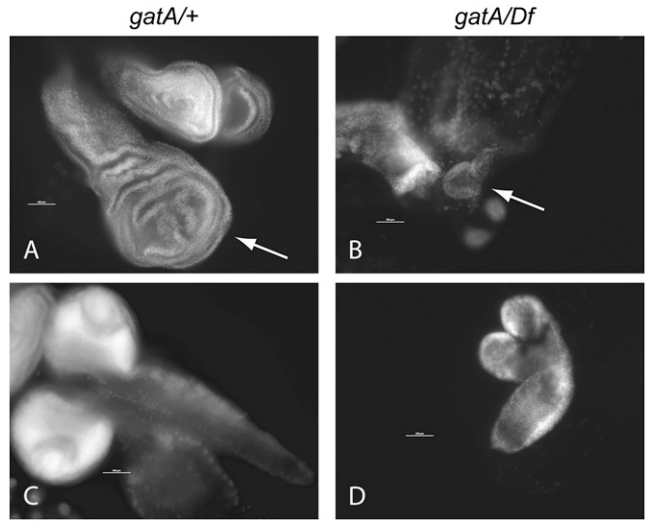

FIGURE 2.—Growth defects in mitotic tissues in 5-day-AEL *gatA* larvae. (A–D) 20×, DAPI staining; bars, 200 μm. (A) *gatA*/+ wing disc (arrow) and haltere discs (top right). (B) $gatA^{112}$/*Df* wing disc (arrow). (C) *gatA*/+ brain (D) $gatA^{112}$/*Df* brain.

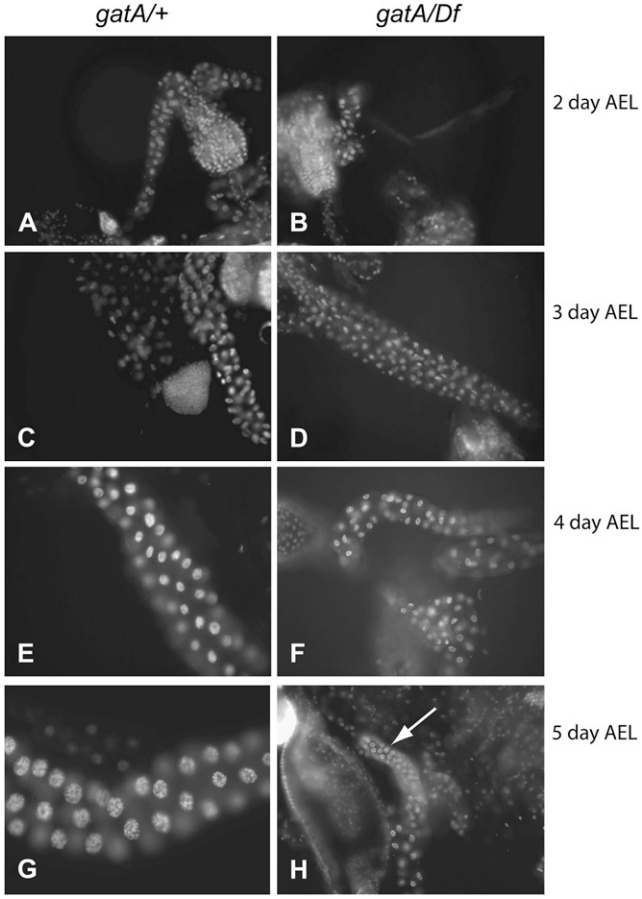

Figure 3.—Growth and DNA content of salivary glands in wild-type and *gatA* larvae. (A–H) 20×, DAPI staining. (A, C, E, and G) *gatA*/+. (B, D, F, and H) $gatA^{112}$/*Df*. (A and B) 2 days AEL. (C and D) 3 days AEL. (E and F) 4 days AEL. (G and H) 5 days AEL. Arrow points to *gatA/Df* salivary gland.

defects. By 3–4 days AEL, salivary gland cells in wild-type larvae are much larger and contain more DNA than salivary gland cells in their *gatA/Df* siblings. One day later, this difference is even more dramatic (Figure 3, A–H). We observed similar differences between wild-type and mutant larvae in all larval tissues (not shown). We observed no obvious defects in chromosome condensation in *gatA* salivary glands in contrast to the chromosome morphology defects that we observed in nurse cells and oocytes in our clonal screen (Morris *et al.* 2003), perhaps because wild-type salivary gland cell chromosomes retain their polyploid organization throughout larval development.

Mapping and molecular identification of *gatA*: The $gatA^{112}$, $gatA^{50}$, and $gatA^{145}$ alleles had been previously mapped to a 300-kb region (91D1-F2) by complementation testing against the 3R deficiency mapping kit (Morris *et al.* 2003). We carried out further complementation testing and found two particularly informative Deficiencies that failed to complement all three *gatA* EMS alleles and the $gatA^{s}$ allele: *Df(3R)Exel6182* and *Df(3R)Exel6183*.

The right breakpoint of *Df(3R)Exel6182* and the left breakpoint of *Df(3R)Exel6183* fall at the same site in the genome (K. Cook, personal communication, FlyBase). *Df(3R)Exel6182* removes the fourth exon of *gatA* (which encodes nearly two-thirds of the protein), as well as the 5′-UTR and approximately the first 10 codons of *NP15.6*. *Df(3R)Exel6183* removes the first three exons of *gatA* and >90% of *NP15.6* (Figure 4). *NP15.6* and *gatA* fall in the densest cluster of unrelated genes in any characterized eukaryote (Misener and Walker 2000). On both the left and right, *gatA* is separated from adjacent genes by ~100 bp. *gatA* has three introns; the first two introns are 53 and 60 bp long, and the third intron, which is 910 bp long, contains the 664-bp intronless gene, *NP15.6* (Figure 4A).

A number of transposon insertions had been mapped to the 300-kb region defined by our initial deficiency mapping. We tested these insertions and found that *P{neoFRT}82B P{lacW}l(3)S092902* failed to complement the *gatA* alleles. We molecularly mapped the insertion site by inverse PCR amplification and sequencing of the genomic DNA flanking the *P* element (Bellen *et al.* 2004). The transposon separates the first three exons of *gatA* from the large fourth exon. The insertion also separates the first eight codons of *NP15.6*, including the only methionine codon, from the rest of the gene (Figure 4A).

Since deficiency mapping and molecular identification of the $gatA^{s}$ insertion site implicated *gatA* or *NP15.6* in our mutants, we sequenced both genes in our EMS alleles. All three alleles showed no base changes in *NP15.6*, but each allele showed a single base change predicted to severely disrupt *gatA* (Figure 5 and see below). $gatA^{50}/gatA^{112}$ *trans*-heterozygotes show the same phenotypes as *gatA/Df* (Figure 4, B–E), indicating that point mutations in *gatA* cause the growth defects that we observed. To rule out the possibility that the *gatA* EMS alleles reduce *NP15.6* expression in addition to disrupting *gatA* translation, we carried out Northern blot analysis on *gatA*/+ and $gatA^{50}/gatA^{112}$ larvae (Figure 4F). The *trans*-heterozygous larvae express *NP15.6* strongly, indicating that these point mutants affect only *gatA*. Taken together, our mapping, allele sequencing, mRNA expression, and phenotypic analysis data show that mutations in *gatA* are responsible for the phenotypes that we observe in our *gatA* mutants. The similarity in phenotypes of the EMS and transposon alleles in *trans* to each other or to the deficiency, along with our molecular characterization of the alleles (see below), leads us to believe that the alleles are null.

***gatA* sequence analysis:** All three *gatA* EMS alleles showed single base changes in *gatA*. None showed a change in *NP15.6*. $gatA^{145}$ encodes a nonsense mutation at 145W. $gatA^{112}$ encodes a nonsense mutation at 154W. The $gatA^{50}$ mutation is a T-to-A substitution in the donor splice site of intron 3 (Figure 5). If the intron fails to splice, an in-frame translational stop occurs at the 46th codon within the intron. It is possible that the mutant

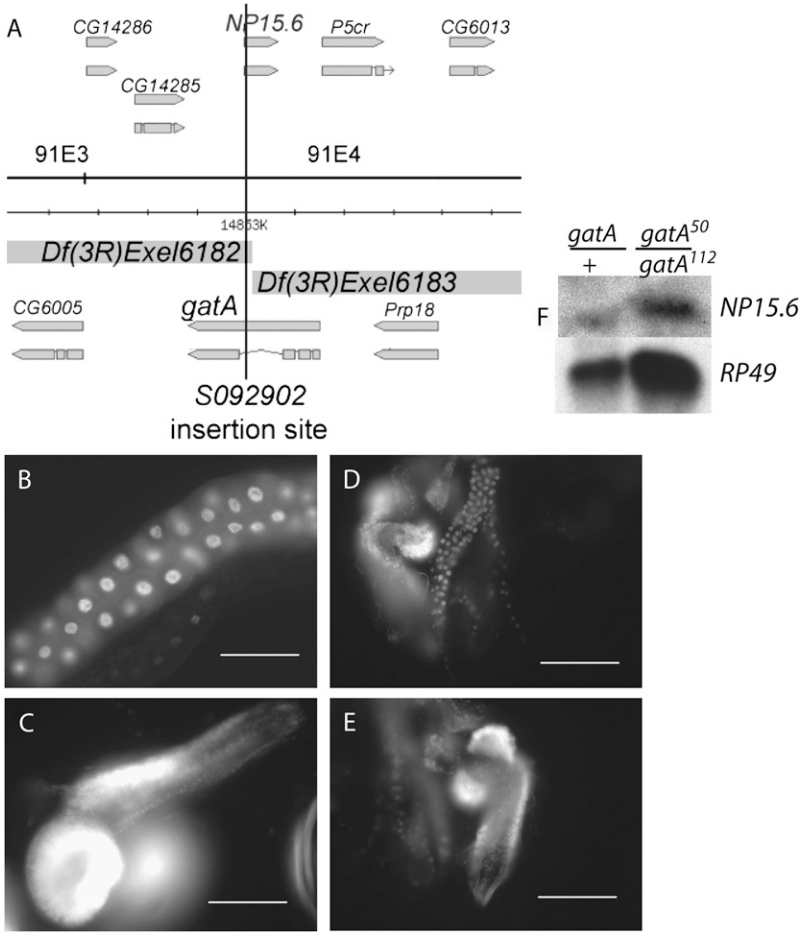

FIGURE 4.—Mapping and identification of *gatA* as the gene disrupted in all *bene* alleles. (A) *Df(3R)Exel6182* and *Df(3R)Exel6183* extend in opposite directions from a shared breakpoint at the insertion site of P{XP}d03824, which falls at bp 14,853,107 (K. COOK, FlyBase, personal communication). The P insertion *P{lacW}l(3)S092902* was previously mapped by cytology to 91F1-F2. We mapped the insertion site molecularly, using inverse PCR (see MATERIALS AND METHODS), to the third intron of *gatA* between codons 8 and 9 of *NP15.6*. Gene positions and splice forms adapted from FlyBase (GRUMBLING and STRELETS 2006). (B–E) DAPI stainings of tissues in 5-day-AEL *gatA*/+ and $gatA^{50}/gatA^{112}$ *trans*-heterozygotes. (B and C) *gatA*/+. (D and E) $gatA^{50}/gatA^{112}$. (B and D) salivary gland. (C and E) Brain. (F) Northern blot showing strong *NP15.6* expression in *gatA*/+ and $gatA^{50}/gatA^{112}$. *RP49* is the loading control.

transcript may use a cryptic splice site, but we would not predict protein translated from the mutant allele to have significant activity, since the allele is genetically null. The GatA amino acid sequence is highly conserved, including extensive regions that fall after the stop codons in the mutants. Drosophila and human *gatA* share 53% amino acid identity. Drosophila and yeast *gatA* share 29% identity. Drosophila and cyanobacteria *gatA* share 39% identity. The EMS alleles and the P insertion are therefore strong candidates for molecular null alleles.

***gatA* expression and cell autonomy:** *gatA* is the only obvious candidate for the mitochondrial glutamyl-tRNA(Gln) amidotransferase subunit A gene in the Drosophila genome. The genome includes several other amidotransferases, but their sequences disqualify them as candidate *gatA* orthologs. We would therefore predict *gatA* to be required in all cells. We generated *gatA* mutant clones in eye imaginal discs by crossing *w, ey-FLP; FRT, Rps3, P{ubi-GFP, w+}/TM6B* females by *FRT e gatA/TM3, Sb, kr-GFP* males. The *Rps3* allele is recessive cell-lethal and has a subtle dominant growth phenotype (Figure 6, A and B). *gatA/TM6B* eyes are wild type, as expected (Figure 6, C and G), but $gatA^{112}$ and $gatA^{50}$ mutant clones show several defects (Figure 6, D, E, F, and H). Eyes with *gatA* clones are small and misshapen and show various differentiation defects, including cuticle scars, ectopic bristles, rough eyes, and failure to develop ommatidia. The *gatA* growth defects that we observed in larvae are therefore not likely to be due to defects in a single organ (*e.g.*, the brain), which would arrest growth in the whole organism. Instead, mutant tissues autonomously exhibit growth defects. Consistent with our prediction that every tissue would require *gatA* activity, RT–PCR analysis of wild-type tissues shows *gatA* expression in a wide range of mitotic and endoreplicating tissues, including larval gut, imaginal disc, fat body, salivary gland, and adult ovary (Figure 6I)

DISCUSSION

gatA function is required cell-autonomously in the germ cells of the ovary for endoreplication-associated growth and DNA accumulation and for proper chromosome morphology. We have shown here that the $gatA^{112}$, $gatA^{145}$, and $gatA^{50}$ EMS alleles and the $gatA^{S}$ transposon insertion allele are all predicted to result in early stop codons or splicing defects in the *gatA* gene. Homozygous $gatA^{S}$ mutations and all mutant *gatA* alleles in *trans* to the deficiency cause similar phenotypes;

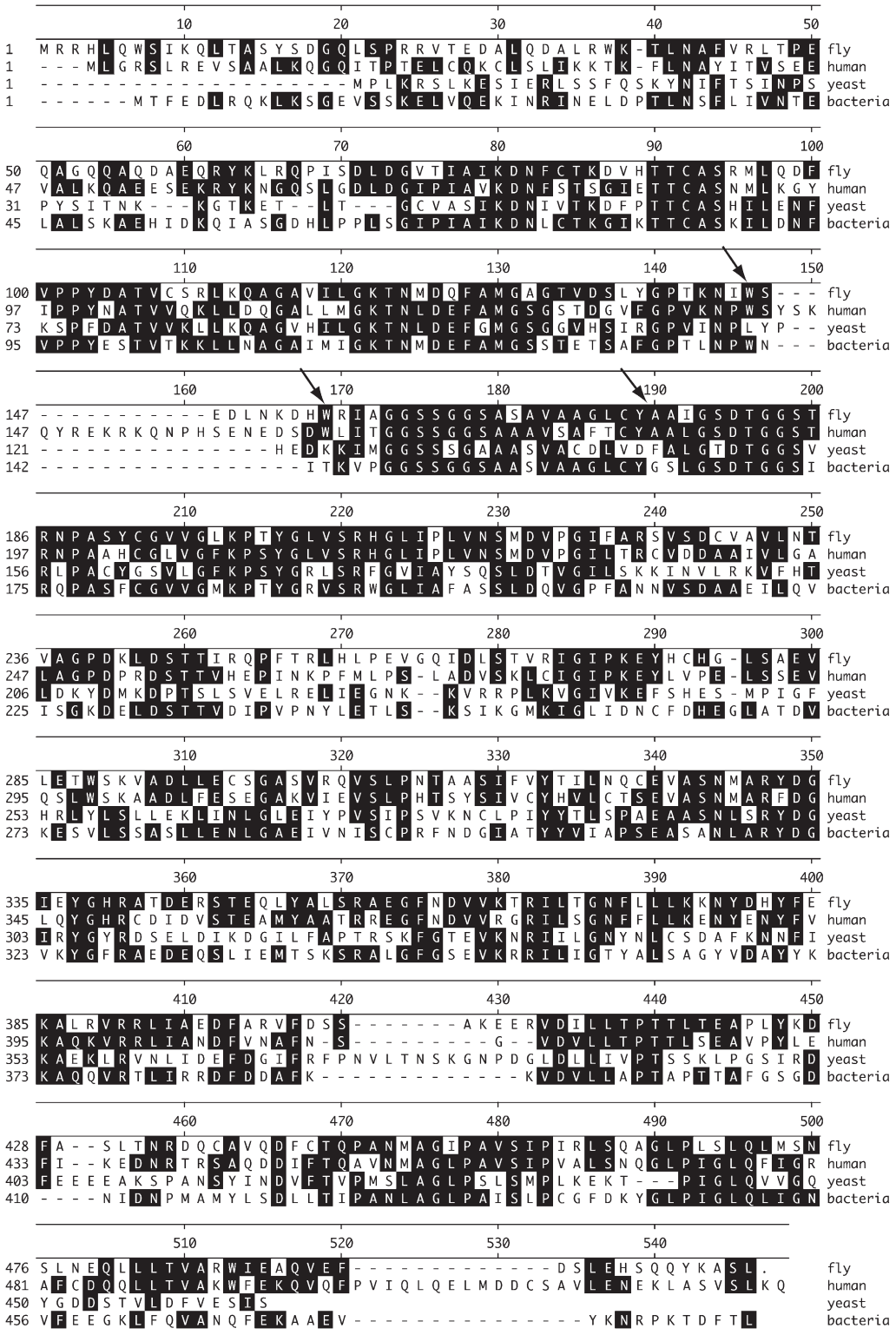

Figure 5.—ClustalW alignment of Drosophila GatA protein sequence with GatA sequences from other species. Accession numbers are as follows: fly—NP_650775.2; human—CAB66614; yeast (*S. cerevisiae*)—Q03557; bacteria (the cyanobacteria, *Prochlorococcus marinus*)—YP_291459. Arrows signify lesions in *gatA* point mutants. $gatA^{145}$, W145STOP; $gatA^{112}$, W154STOP; $gatA^{50}$, T-A substitution in intron donor sequence, predicted to disrupt splicing between 174Y and 175A.

the alleles therefore fulfill the criteria for genetic and molecular nulls. Both the mitotic and endoreplicating tissues in *gatA* larvae are small, and the larvae die before pupariation. The endoreplicating nuclei exhibit much lower DNA contents but appear otherwise normal, suggesting that the mutant endocycle is slower or less efficient. As in the germ cells of the ovary, *gatA* is required autonomously in the cells of the eye for normal growth and differentiation, and *gatA* is expressed very broadly throughout the larva, as we would expect of a gene required for mitochondrial function.

Function of *gatA*: In the cytoplasm of eukaryotic cells, different tRNA synthetases are used to charge the appropriate tRNAs with each of the 20 amino acids

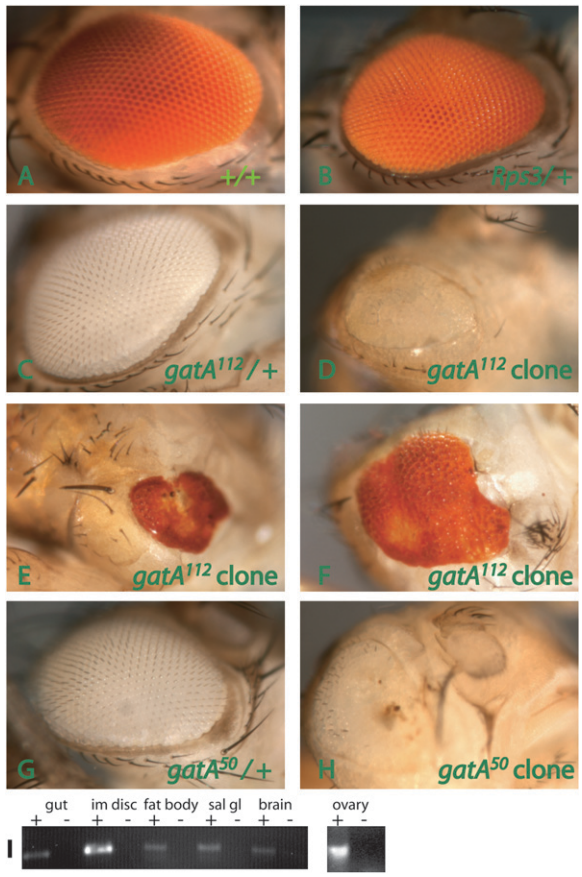

FIGURE 6.—Mosaic analysis and expression of *gatA*. *w, ey-FLP, Gla-lacZ; FRT Rps3, P{ubi-GFP, w+}/TM6B* females were crossed with *FRT e gatA*^{50}*/TM3, Sb* males, *FRT e gatA*^{112}*/TM3, Sb* males or *FRT +/TM3, Sb* males. (A–H) Adult eyes. The *FRT Rps3* chromosome carries a *w*+ transgene. *Rps3* is recessive cell lethal. Therefore, in males, cells that have not undergone recombination are yellow. Cells that have recombined are white (homozygous for + or *gatA*, depending on the cross). (A, B, E, and F) Female eyes are *w*+, aiding phenotypic analysis, but making it difficult to determine the genotype of cells. (C, D, G, and H) Male eyes are *w*–, permitting easy genotyping of eye clones. (A) Wild-type clone shows normal growth and development. (B) *Rps3*/+ eyes (no clones induced) are slightly smaller than wild type. (C) *gatA*^{112}/+ eyes (no clones induced) and (G) *gatA*^{50}/+ eyes (no clones induced) are normal. (D–F) *gatA*^{112} clones and (H) *gatA*^{50} clones cause small, misshapen eyes with cuticle scars and ectopic bristles. There is a small, pale yellow region in the top portion of the eye in D, because ey-FLP induced mitotic recombination somewhat late in this eye. (I) RT–PCR of *gatA* from RNA extracts from larval gut (lanes 1 and 2), imaginal discs (lanes 3 and 4), fat bodies (lanes 5 and 6), salivary gland (lanes 7 and 8), brain (lanes 9 and 10), and from adult ovary (separate gel, lanes 11 and 12). "+" and "−" refer to treatment of extracts with reverse transcriptase.

encoded in the genome. In many eubacteria, as well as in mitochondria and chloroplasts and many archeabacteria, there is no dedicated tRNA synthetase for Gln tRNAs analogous to the Gln tRNA synthetases present in eukaryotic genomes. Instead, in what is believed to be the more ancient process, both Gln and Glu tRNAs are initially charged with glutamic acid. The glutamic acid misacylated to Gln tRNA [Glu-tRNA(Gln)] then undergoes an amidotransferase reaction catalyzed by glutamyl-tRNA(Gln) amidotransferase (RAJBHANDARY 1997). The A and B subunits of this heterodimeric enzyme are encoded by *gatA* and *gatB*, respectively (CURNOW *et al.* 1997). In archeabacteria, GatD and GatE carry out the amidotransferase reactions on Gln tRNAs (FENG *et al.* 2005). Although GatA proteins are highly conserved in prokaryotes, fungi, and animals, the *gatA* alleles described here are the first reported eukaryotic *gatA* mutants. The only other characterized eukaryotic mutants in this pathway are defective in *Saccharomyces cerevisiae pet112*. Intriguingly, *pet112* cells are small, but viable. The petite phenotype can be complemented by *Bacillus subtilis gatB* (KIM *et al.* 1997). This suggests that the *gatA* growth/cell cycle defects that we observed in Drosophila may reflect an evolutionarily conserved requirement for normal mitochondrial physiology for cell cycle and growth control.

TABLE 1

Polypeptides encoded by the Drosophila mitochondrial genome

Protein	Composition	Complex
ND1	5 Gln/312 aa	I
ND2	7 Gln/341 aa	I
ND3	1 Gln/117 aa	I
ND4	6 Gln/446 aa	I
ND4L	1 Gln/96 aa	I
ND5	10 Gln/574 aa	I
ND6	3 Gln/174 aa	I
CytB	8 Gln/378 aa	III
COX1	10 Gln/511 aa	IV
COX2	7 Gln/228 aa	IV
COX3	7 Gln/262 aa	IV
ATP6	4 Gln/224 aa	V
ATP8	1 Gln/53 aa	V

Mitochondrial mutant phenotypes: Mitochondria are complex organelles responsible for the production of NADH, $FADH_2$, and ATP via the Krebs cycle and the transfer of electrons from NADH to oxygen via the electron transport chain. In addition, mitochondria regulate transport across their membranes, replicate their genomes, and transcribe and translate their own mRNAs and proteins. Although mitochondria require hundreds of proteins to carry out their diverse functions, almost all animal mitochondrial proteins are encoded in the nuclear genome and translated in the cytoplasm. The 13 protein-encoding genes in the animal mitochondrial genome all participate in the various complexes involved in electron transfer (Table 1).

GatA is one of the mitochondrial proteins encoded in the nuclear genome. *gatA* loss of function could result in one of two possible outcomes, either of which would

affect all 13 of the proteins encoded in the mitochondrial genome. One possible outcome would be that all glutamines would be mistranslated as glutamates, which, for some of the highly conserved proteins that contain multiple glutamine codons, would likely result in inactive proteins (Table 1). Another possibility, suggested by data from chloroplast translation, would be that translation of all the proteins would simply fail. Misacylated Glu-tRNA(Gln) in chloroplasts is not brought to the ribosome by Ef-Tu, so it cannot participate in translation (Stanzel *et al.* 1994). It is not known whether mitochondrial translation functions similarly. Either likely effect of *gatA* loss of function would render aerobic respiration impossible.

A number of interesting genetic and pharmacological studies of flies compromised in aerobic respiration have been published. Drosophila grown under hypoxic conditions grow poorly, although they upregulate glycolysis sufficiently to survive (Digregorio *et al.* 2001; Frazier *et al.* 2001; Frei *et al.* 2005). Consistent with our observations of growth defects in *gatA* mutants, loss of function in the mitochondrial protein translocator component gene, *tim50*, causes growth and cell cycle defects in Drosophila larvae (Sugiyama *et al.* 2007). *bonsai* mutants, like *gatA* mutants, exhibit growth defects, although even *bonsai* null animals can develop into small adults (Galloni 2003). Possibly, loss of *bonsai*, which encodes a mitochondrial ribosomal protein, is less deleterious than loss of *gatA*. Arguing in favor of this model, *bonsai* expression after early embryonic development appears restricted to the gut, suggesting that most tissues do not require high levels of Bonsai (Galloni 2003).

In contrast to the growth defects observed in *gatA* and *tim50* mutants, later or more subtle defects in aerobic respiration primarily affect nerve and muscle function. Late exposure to electron transport inhibitors such as the complex I inhibitor, rotenone, or the complex III inhibitor, antimycin, causes nervous system defects (Miwa and Brand 2003; Coulom and Birman 2004; Frei *et al.* 2005). Similarly, weak loss-of-function mutations in, for example, the mitochondrial ribosomal protein, *tko* (Royden *et al.* 1987), or in the complex V component, *ATP6* (Celotto *et al.* 2006), permit flies to reach adulthood with significant muscle and/or nervous system defects. The fact that null alleles of the mitochondria-associated ubiquitin E3 protein ligase, *parkin*, cause adult muscular defects rather than larval lethality and growth defects (Greene *et al.* 2003) may suggest that *parkin* is not required for mitochondrial activity in all tissues.

One interesting question is how *gatA* larvae manage to survive and grow as well as they do, given the importance and broad expression pattern of *gatA*. Possibly, the early *gatA* survival should be attributed to the fly's remarkable capacity to rely on glycolysis for most of its energy requirements (Digregorio *et al.* 2001). Very likely, *gatA* embryos and early larvae also benefit from maternal rescue via maternally contributed mitochondria and *gatA* mRNA, consistent with our detection of *gatA* expression in ovaries (Figure 6I).

Permissive *vs.* instructive role for mitochondrial mutants in growth: The mitochondrial genes required for normal growth, including *gatA*, may act permissively, merely providing energy required for increasing cell numbers and/or cell size. Alternatively, the growth genes may play an instructive role, such that cells experiencing metabolic defects actively reallocate resources away from growth and toward pathways and behaviors appropriate to survival under suboptimal conditions. We do not yet know whether *gatA* mutants specifically downregulate growth pathways, although several lines of evidence suggest that they might. Mitochondrial malfunction has been shown to arrest growth by interfering specifically with cell cycle and cell size regulators. Cells in flies grown under hypoxic conditions or in the presence of the electron transport chain inhibitor, cyanide, arrest at specific points in the cell cycle (Digregorio *et al.* 2001). Diploid cells homozygous for null mutations in *tenured*, which encodes the ATP synthase component, Cox Va, arrest at the G_1-S checkpoint by repressing CycE in a p53-dependent manner (Mandal *et al.* 2005). Since control of CycE is sufficient to regulate the endocycle (Lilly and Duronio 2005), this mitochondrial checkpoint might explain growth defects in endoreplicating tissues as well. CycD/Cdk4 control of growth also depends on mitochondrial genes. CycD/Cdk4 activation stimulates mitochondrial activity and induces Hif-1 prolyl hydroxylase to signal cell growth. Both of these functions require the mitochondrial ribosomal protein mRpL12 (Frei *et al.* 2005).

In addition to the mitochondrial protein–cyclin interactions described above, the specificity of the *gatA* phenotypes argues that the growth defects in *gatA* larvae should not be attributed simply to running out of energy. *gatA* mutant larvae continue to move and forage for days after they cease growing, suggesting mitochondrial dysfunction in *gatA* mutants may instruct the cell to reallocate resources away from growth before the animal has entirely depleted its energy stores. In the ovary, chromosome condensation and chromosome morphology are defective in *gatA* mutants long before the egg chambers die, possibly indicating cell cycle or DNA repair defects in *gatA* mutants (Morris *et al.* 2003). It would be interesting to learn if these defects are related to chromosome condensation defects reported in Drosophila embryos that were grown under hypoxic conditions (Foe and Alberts 1985) and if other mutations that cause chromosome morphology defects in egg chambers are also defective in aerobic respiration.

The authors gratefully acknowledge R. Lehmann and J. Treisman for their generosity in giving us access to their microscopes and fly kitchen; Vanessa Flores, Christopher O'Connor, and Jane Mueller for assistance with experiments; and L. Gilboa, C. Navarro, and M. Morris

for their feedback and support. We thank Kevin Legent for technical advice concerning the eye clones experiment. We also thank the R. Lehmann, J. Treisman, and L. Johnston labs and the Bloomington and Szeged stock centers for providing the fly stocks used in this research. This work was supported by National Institutes of Health R15 Award GM074735-01 and by a Fordham Faculty Research Grant.

LITERATURE CITED

Altschul, S. F., W. Gish, W. Miller, E. W. Myers and D. J. Lipman, 1990 Basic local alignment search tool. J. Mol. Biol. **215:** 403–410.

Bellen, H. J., R. W. Levis, G. Liao, Y. He, J. W. Carlson *et al.*, 2004 The BDGP gene disruption project: single transposon insertions associated with 40% of Drosophila genes. Genetics **167:** 761–781.

Britton, J. S., W. K. Lockwood, L. Li, S. M. Cohen and B. A. Edgar, 2002 Drosophila's insulin/PI3-kinase pathway coordinates cellular metabolism with nutritional conditions. Dev. Cell **2:** 239–249.

Celotto, A. M., A. C. Frank, S. W. McGrath, T. Fergestad, W. A. Van Voorhies *et al.*, 2006 Mitochondrial encephalomyopathy in Drosophila. J. Neurosci. **26:** 810–820.

Chenna, R., H. Sugawara, T. Koike, R. Lopez, T. J. Gibson *et al.*, 2003 Multiple sequence alignment with the Clustal series of programs. Nucleic Acids Res. **31:** 3497–3500.

Coelho, C. M., B. Kolevski, C. D. Walker, I. Lavagi, T. Shaw *et al.*, 2005 A genetic screen for dominant modifiers of a small-wing phenotype in *Drosophila melanogaster* identifies proteins involved in splicing and translation. Genetics **171:** 597–614.

Coulom, H., and S. Birman, 2004 Chronic exposure to rotenone models sporadic Parkinson's disease in Drosophila melanogaster. J. Neurosci. **24:** 10993–10998.

Curnow, A. W., K. Hong, R. Yuan, S. Kim, O. Martins *et al.*, 1997 Glu-tRNAGln amidotransferase: a novel heterotrimeric enzyme required for correct decoding of glutamine codons during translation. Proc. Natl. Acad. Sci. USA **94:** 11819–11826.

DiGregorio, P. J., J. A. Ubersax and P. H. O'Farrell, 2001 Hypoxia and nitric oxide induce a rapid, reversible cell cycle arrest of the Drosophila syncytial divisions. J. Biol. Chem. **276:** 1930–1937.

Edgar, B. A., 2006 How flies get their size: genetics meets physiology. Nat. Rev. Genet. **7:** 907–916.

Edgar, B. A., and T. L. Orr-Weaver, 2001 Endoreplication cell cycles: more for less. Cell **105:** 297–306.

Feng, L., K. Sheppard, D. Tumbula-Hansen and D. Soll, 2005 Gln-tRNAGln formation from Glu-tRNAGln requires cooperation of an asparaginase and a Glu-tRNAGln kinase. J. Biol. Chem. **280:** 8150–8155.

Foe, V. E., and B. M. Alberts, 1985 Reversible chromosome condensation induced in Drosophila embryos by anoxia: visualization of interphase nuclear organization. J. Cell Biol. **100:** 1623–1636.

Frazier, M. R., H. A. Woods and J. F. Harrison, 2001 Interactive effects of rearing temperature and oxygen on the development of Drosophila melanogaster. Physiol. Biochem. Zool. **74:** 641–650.

Frei, C., M. Galloni, E. Hafen and B. A. Edgar, 2005 The Drosophila mitochondrial ribosomal protein mRpL12 is required for cyclin D/Cdk4-driven growth. EMBO J. **24:** 623–634.

Galloni, M., 2003 Bonsai, a ribosomal protein S15 homolog, involved in gut mitochondrial activity and systemic growth. Dev. Biol. **264:** 482–494.

Galloni, M., and B. A. Edgar, 1999 Cell-autonomous and non-autonomous growth-defective mutants of Drosophila melanogaster. Development **126:** 2365–2375.

Greene, J. C., A. J. Whitworth, I. Kuo, L. A. Andrews, M. B. Feany *et al.*, 2003 Mitochondrial pathology and apoptotic muscle degeneration in Drosophila parkin mutants. Proc. Natl. Acad. Sci. USA **100:** 4078–4083.

Grumbling, G., and V. Strelets, 2006 FlyBase: anatomical data, images and queries. Nucleic Acids Res. **34:** D484–D488.

Kim, S. I., N. Stange-Thomann, O. Martins, K. W. Hong, D. Soll *et al.*, 1997 A nuclear genetic lesion affecting Saccharomyces cerevisiae mitochondrial translation is complemented by a homologous Bacillus gene. J. Bacteriol. **179:** 5625–5627.

Lambertsson, A., 1998 The minute genes in Drosophila and their molecular functions. Adv. Genet. **38:** 69–134.

Li, J., and W. X. Li, 2006 A novel function of Drosophila eIF4A as a negative regulator of Dpp/BMP signalling that mediates SMAD degradation. Nat. Cell Biol. **8:** 1407–1414.

Lilly, M. A., and R. J. Duronio, 2005 New insights into cell cycle control from the Drosophila endocycle. Oncogene **24:** 2765–2775.

Mandal, S., P. Guptan, E. Owusu-Ansah and U. Banerjee, 2005 Mitochondrial regulation of cell cycle progression during development as revealed by the tenured mutation in Drosophila. Dev. Cell **9:** 843–854.

Misener, S. R., and V. K. Walker, 2000 Extraordinarily high density of unrelated genes showing overlapping and intraintronic transcription units. Biochim. Biophys. Acta **1492:** 269–270.

Miwa, S., and M. D. Brand, 2003 Mitochondrial matrix reactive oxygen species production is very sensitive to mild uncoupling. Biochem. Soc. Trans. **31:** 1300–1301.

Morris, J. Z., C. Navarro and R. Lehmann, 2003 Identification and analysis of mutations in bob, Doa and eight new genes required for oocyte specification and development in *Drosophila melanogaster.* Genetics **164:** 1435–1446.

RajBhandary, U. L., 1997 Once there were twenty. Proc. Natl. Acad. Sci. USA **94:** 11761–11763.

Royden, C. S., V. Pirrotta and L. Y. Jan, 1987 The tko locus, site of a behavioral mutation in D. melanogaster, codes for a protein homologous to prokaryotic ribosomal protein S12. Cell **51:** 165–173.

Saucedo, L. J., and B. A. Edgar, 2007 Filling out the Hippo pathway. Nat. Rev. Mol. Cell Biol. **8:** 613–621.

Stanzel, M., A. Schon and M. Sprinzl, 1994 Discrimination against misacylated tRNA by chloroplast elongation factor Tu. Eur. J. Biochem. **219:** 435–439.

Sugiyama, S., S. Moritoh, Y. Furukawa, T. Mizuno, Y. M. Lim *et al.*, 2007 Involvement of the mitochondrial protein translocator component tim50 in growth, cell proliferation and the modulation of respiration in Drosophila. Genetics **176:** 927–936.

Weinkove, D., and S. J. Leevers, 2000 The genetic control of organ growth: insights from Drosophila. Curr. Opin. Genet. Dev. **10:** 75–80.

Communicating editor: T. C. Kaufman